

# **A method of the atomized fluid hologram analysis in examinations of atomization spectrum**

MIROSLAW WĘCLAŚ

Institute of I.C. Engines, Technical University of Poznań, 60-965 Poznań, Piotrowo 3, Poland.

The quality of the results obtained in holographic examination of the fluid streams depends significantly on the choice of a suitable method of the hologram analysis. In this paper, a method for the choice of measurement zones and the analysis of atomized water made according to the tunneling principle are presented. Attention is paid to the droplet agglomeration zone at the fluid atomizer outlet and to the turbulent perturbation of the stream front, which make impossible the analysis of droplets in these regions. The results reported concern the atomization of water from the whirling injector and having, in particular, in mind the analysis of atomization spectrum. Atomization spectrum and numerical force of the population, depending on the distance from the injector, were analysed for two sizes of the injectors and three values of the feeding pressure and presented graphically. In the presented distributions of spectra distinct local maxima can be observed. In this work, the analysis of the atomization in practical problems, given in the paper, is exemplified by a compression-ignition engine of direct injection. The application of a holographic system, to the fuel atomization examination in a combustion chamber of a working engine, was also proposed.

## **1. Introduction**

At present, the laser holography is the most perfect tool for analysis of small particles, being even superior to the so far used photographic techniques. Holography is a non-destructive (no touch) optical method, enabling an efficient examination of the real course of atomization process. Moreover, in contrast to the photographic methods, it offers the possibility of recording the particles (droplets) of large volume of the stream. The depth of view, while taking a hologram of the volume filled with droplets, amounts to several centimeters for the droplet diameters, ranging from few micrometers up to several thousands micrometers. The laser holography is a method of a quick and pulsed recording of small particles. At the present time, when there are no technical difficulties in recording the hologram of droplets, the methodology of its analysis concerning the quality and the value of the obtained results becomes an important problem. This problem, being presented and interpreted by different authors in different ways [1-3] has not been solved uniquely, yet.

In this work, the author presents the methods of hologram analysis and measurement of droplets, the latter one being then compared with those described in the literature [1, 2, 4, 5].

## 2. Atomization spectrum

The droplets are considered as a statistical ensemble in which, due to the spherical shape of the droplets, the droplet diameter  $\Phi$  is accepted as a random variable  $x$  over this ensemble. Below, the atomization spectrum analysis will be discussed. On the basis of mathematical statistics by atomization spectrum we mean the relationship between the population frequency  $\Delta n_i$  of the droplets lying within the interval of diameters  $\langle x_i - \Delta x/2, x_i + \Delta x/2 \rangle$  and the diameter  $x_i$  ( $x_i$  is the diameter corresponding to the midpoint of each  $i$ -th interval, while  $\Delta x$  denotes the constant width of the interval).

Next, we will introduce and define several notions characterizing the atomization spectrum.

i) Population frequency

$$N = \sum_{i=1}^{i=m} \Delta n_i \quad (1)$$

where  $m$  - number of diameter intervals.

ii) Quantitative frequency of the droplets within the given interval, the latter being frequency of the  $i$ -th ensemble referred to the total frequency of the ensemble, calculated according to Eq. (1)

$$\Delta \hat{n}_i = \frac{\Delta n_i}{N} = \frac{\Delta n_i}{\sum_{i=1}^{i=m} \Delta n_i}. \quad (2)$$

iii) Function of quantitative distribution of droplets. When treating the random variable  $x$  to be continuous inside the measurement region  $\langle x_{\min}, x_{\max} \rangle$  we may write

$$f_n(x) = \frac{d\hat{n}}{dx} \frac{dn/dx}{\int_{x_{\min}}^{x_{\max}} (dn/dx) dx}. \quad (3)$$

iv) Distribution function of the random variable  $x$

$$\Omega_n(x) = \sum_{i=1}^{i=m} \Delta \hat{n}_i. \quad (4)$$

v) Average diameter of the droplets

$$\Phi_{pq} = x_{pq} = \sqrt[p-q]{\frac{\sum_{i=1}^{i=m} x_i^p \Delta n_i}{\sum_{i=1}^{i=m} x_i^q \Delta n_i}}. \quad (5)$$

Depending on the assumed values of  $p$  and  $q$  the following equivalent diameters, essential for the analysis of spectrum ( $p > q$ ), may be distinguished:

– average surface diameter

$$\Phi_{20} = \sqrt{\frac{\sum x^2 \Delta n}{\sum \Delta n}}, \quad p = 2, \quad q = 0, \quad (6)$$

– average volume diameter

$$\Phi_{30} = \sqrt[3]{\frac{\sum x^3 \Delta n}{\sum \Delta n}}, \quad p = 3, \quad q = 0, \quad (7)$$

– relative surface diameter

$$\Phi_{21} = \frac{\sum x^2 \Delta n}{\sum x \Delta n}, \quad p = 2, \quad q = 1, \quad (8)$$

– relative volume diameter

$$\Phi_{31} = \sqrt[3]{\frac{\sum x^3 \Delta n}{\sum x \Delta n}}, \quad p = 3, \quad q = 1, \quad (9)$$

– average Sauter diameter ( $\Phi_S = \Phi_{32}$ )

$$\Phi_S = \frac{\sum x^3 \Delta n}{\sum x^2 \Delta n}, \quad p = 3, \quad q = 2. \quad (10)$$

### 3. Theoretical fundamentals of holographic recording of droplets

It is assumed after [1] and [6] that, due to recording the whole volume of the stream on the hologram, the holograms of droplets are of Fourier type. Under such assumptions the interference fringes coming from particular droplets are superimposed to only a slight degree. Thus, during the reconstruction, the features of the whole population of the holographically recorded droplets may be determined by considering the image of a simple droplet. On the other hand, it should be remembered that the considered type of hologram is similar to Fraunhofer hologram, due to the relation between the distance of the holographic plate from the particle of maximal diameter  $\Phi$  and the magnitude  $\Phi^2/\lambda$ , in the form

$$D > \frac{\Phi^2}{\lambda} \quad (11)$$

where  $\lambda$  – wavelength of the laser light used for recording of the hologram.

The droplets analysed in this work did not exceed several micrometers, thus the assumption of Fraunhofer nature of the hologram is practically justified. For a droplet of diameter  $\Phi$  the intensity distribution recorded on a holographic

plate is described by the expression

$$I(x) = 1 - \frac{k_1 \Phi^2}{2z_1} \sin \frac{k_2 |x|^2}{2z_1} J_1 \left( \frac{k_1 \Phi |\mathbf{x}|}{2z_1} \right) + \frac{k_1^2 \Phi^4}{16z_1^2} \left[ J_1 \left( \frac{k_1 \Phi |\mathbf{x}|}{2z_1} \right) \right]^2 \quad (12)$$

where:  $J_1$  – Bessel function of first kind and first order,

$k_1$  – wavenumber for laser light used during recording,

$z_1$  – distance between the plane of the droplet and the hologram.

The basic problem in the case of the holograms considered, both of Fourier and Fraunhofer types, is the fidelity of the reconstruction of the image. If the effective surface of the hologram is of diameter  $D_h$ , and the droplet image appears at the distance  $z_3$  from the hologram surface, the radius of the Airy disc describing the spread of a geometric object point in the plane of the droplet image amounts to

$$R_0 = 1.22 \frac{\lambda_2 z_3}{D_h}, \quad (13)$$

where  $\lambda_2$  – wavelength of the laser light used for hologram reconstruction. On the other hand, the radius of the Airy disc appearing in the hologram plane due to the object beam diffraction and corresponding to the droplet of the diameter  $\Phi$  located at the distance  $z_1$  from the hologram plane is

$$R_1 = 1.22 \frac{\lambda_1 z_1}{\Phi}. \quad (14)$$

If for the recording and the reconstruction of the hologram a plane wave is used, the minimal diameter of the hologram is  $D_p = 2R$  according to [7], and  $D_{th} = 8R$ , according to [8]. Therefore, the following formulas may be written:

$$D_p = 2.44 \frac{\lambda_1 z}{\Phi}, \quad (15)$$

$$D_{th} = 9.76 \frac{\lambda_1 z}{\Phi}. \quad (16)$$

For the case, when the plane wave is used for both the recording and reconstruction, we have  $z_1 = z_3 = z$ , and the spread of the image of an object point in the hologram plane corresponding to (15) and (16) is, respectively:

$$R_{0p} = 9.5 \mu \Phi, \quad (17)$$

$$R_{0th} = 0.125 \mu \Phi \quad (18)$$

where  $\mu = \lambda_2 / \lambda_1$ .

In the examinations of the water atomization from the whirling atomizer, carried out by the author, the ruby laser light (of the wavelength  $\lambda_1 = 0.6943 \mu\text{m}$ ) was used for the recording and that (of the wavelength  $\lambda_2 = 0.6328 \mu\text{m}$ ) from the He-Ne laser – for the reconstruction. Therefore, for the theoretical diameter

of the droplet  $\Phi = 40 \mu\text{m}$ , the following values of the Airy disc radius were obtained:  $R_{\text{op}} = 18.2284 \mu\text{m}$ ,  $R_{\text{oth}} = 4.5571 \mu\text{m}$ . Thus, the Airy disc calculated according to Thompson is of a diameter twice as small as that calculated according to Pavitt. The recording of holograms of water streams atomized by the whirling atomizers was performed in a two-beam system represented schematically in Fig. 1. The laser beam emerging from the ruby laser falls onto a light-

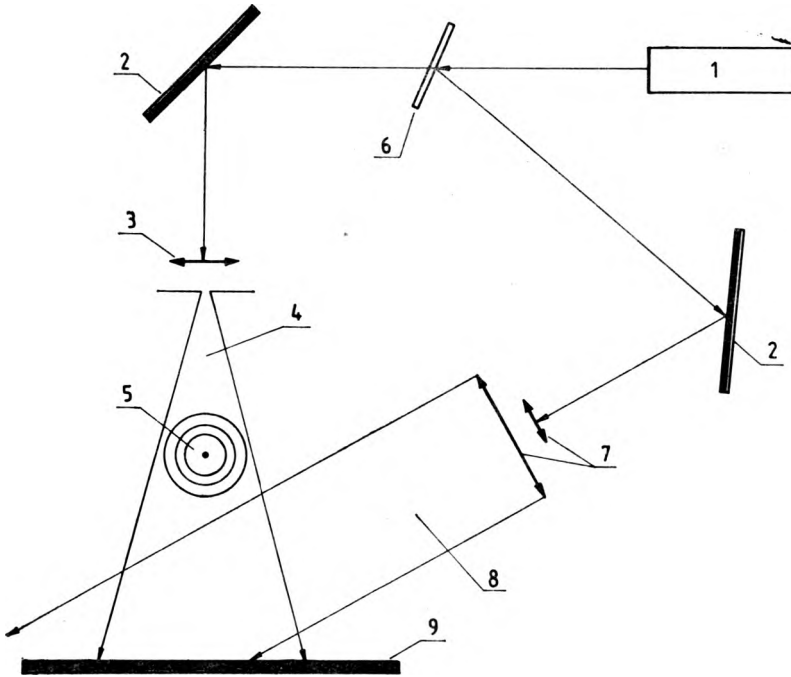


Fig. 1. System for recording the atomized fluid stream on the holographic plate. 1 - ruby laser, 2 - mirror, 3 - pinhole-type aperture lens, 4 - object beam, 5 - fluid stream, 6 - light-splitter, 7 - lens system forming the reference beam, 8 - reference beam, 9 - holographic plate

splitter, where two wave-trains are formed: the reference beam (the wave travelling directly toward the holographic plate) and the object beam, the latter after passing through the examined fluid stream interferes on the holographic plate with the reference beam.

#### 4. Reconstruction and analysis of hologram\*

The fundamental problem in holography of small particles is the reconstruction and analysis of the holograms. Several versions of hologram reconstructing setup are known. The author used the setup shown schematically in Fig. 2.

\* When the hologram is defined as a holographic plate with recorded "frozen" image due to the photochemical processing, the analysis of hologram is reduced to analysis of images reconstructed from the hologram.

In this figure, the images of droplets reconstructed from the hologram are magnified by the microscope and projected via TV camera on the monitor. The author applied the magnifications of order of  $500\times$ . It is believed that it is

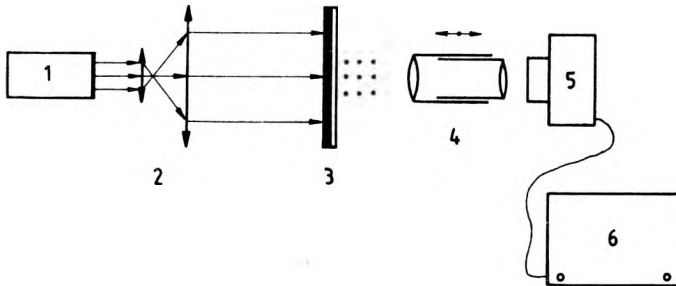


Fig. 2. Droplet hologram reconstruction system with camera and monitor. 1 - laser, 2 - lens system, 3 - hologram, 4 - microscope, 5 - TV camera, 6 - TV monitor

useless to exceed this boundary for the Agfa 10E/75 AH plates, since then the granularity of the background plays the dominant part. A fundamental setup for small particle hologram reconstruction is that proposed by BEXON [9] (Fig. 3). The magnification in this setup may be written in the following way:

$$- \text{ for } z_1 = \mu [1/z_c + 1/(d + z_c) + 1/z_r]^{-1}$$

magnification is

$$M = \frac{d}{z_c} - \mu \frac{d + z_c}{z_r}. \quad (19)$$

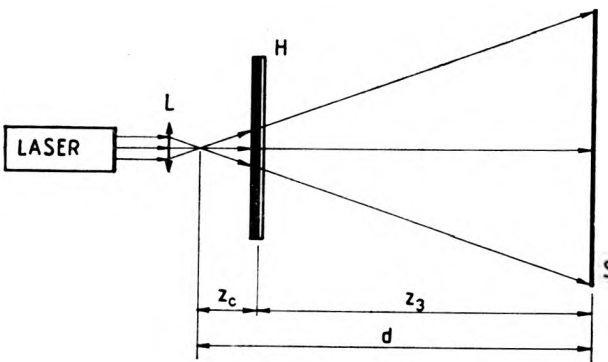


Fig. 3. Bexon system for reconstruction of hologram of small particles [9]. L - lens, H - hologram, S - screen

The author believes, however, that for the examinations discussed in this paper, the Bexon system is practically less useful if compared with the setup from Fig. 2. The Bexon system requires a high accuracy of mutual positioning of the lens, hologram and screen, whereas in the setup proposed by the author the hologram stays at rest, while the position of the microscope is changed axially.

#### 4.1. Analysis of the hologram of the atomized fluid

The basic problem which appears after choosing the method of hologram reconstruction concerns the choice of the measurement zones in the stream and the droplet analysis within the particular zones.

##### 4.1.1. Choice of the measurement zones

The choice of measurement zones according to the so-called tunneling method is presented in Fig. 4. The measurement zones are the planes intersecting the fluid stream perpendicularly to its axis. Within each of the chosen zones either

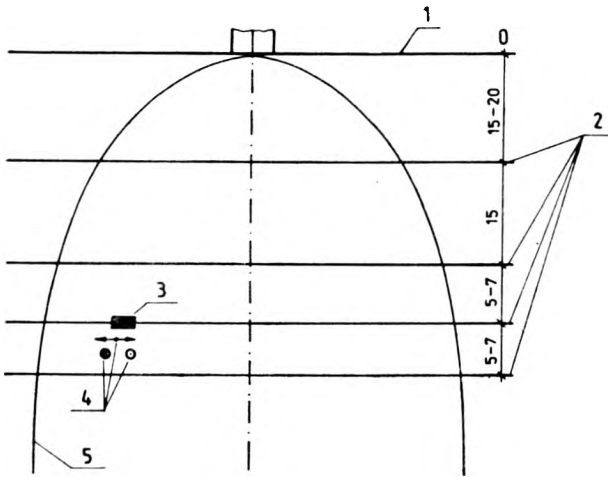


Fig. 4. Selection of the measurement zones on the holographic image of the examined stream: 1 – level of atomizer outlet, 2 – chosen measurement zones, 3 – measurement region ( $1 \times 0.75$  mm), 4 – direction of measurement region movement within a given zone, 5 – stream

a “tunneling” cut of the measurement region of about 1 mm diameter is performed or a tunnel of rectangular 1 mm  $\times$  0.75 mm cross-section is used. Thus, each measurement zone is a set of the measurement regions. It should be noticed that it is necessary to choose the distance between the successive measurement regions within a given measurement zone. The examinations carried out by the author showed that within a given measurement zone the distances between the successive measurement regions should be equal to 1–2 mm. It should be remembered that the analysis in particular measurement regions should be started always with the stream axis proceeding to the left and to the right, separately. Within a given tunnel the analysis of the droplets in-the-depth of the stream in the measurement region should be performed in a continuous way, i.e., all the droplets, being observed, are counted. Also, the principle of one way tunneling should be accepted. It means that in a given tunnel the depth of the read-out may be changed only in one direction (toward the back of the picture plane  $\otimes$  or toward the front of it  $\odot$ ). As it may be noticed from Fig. 3,

the choice of the measurement zones and that of the distances between the particular zones are not accidental, but are subject to certain universal principles and rules. For each type of atomizer, the stream immediately after leaving the holes of the atomizer has not yet fully separated droplets – therefore this part of the stream has been called the zone of droplet glueing. Within this region two or three droplets are glued together taking irregular shapes, therefore sizes and shapes of single droplets cannot be determined. As it results from the author's examinations, it may be assumed that the glueing zone spreads to 15–20 mm from the outlet of the atomizer, while the higher values refer to higher feeding pressure of the atomizer. The next measurement zone should be assumed at the distance of 15 mm from the first one. This zone was called by the author the transition zone, in spite of the fact that the droplets within it are already separated. The successive measurement zones should be assumed at every 5–7 mm distance. The higher values refer to higher feeding pressures of the atomizer. While analysing the droplets in the stream of the atomized fluid, it should be remembered that – due to wave phenomena and turbulent perturbations – a region (analogical to that of droplet glueing) appearing at the stream front is not subject to analysis.

#### 4.1.2. Analysis of droplets

The droplets from the definite sampled volume are recorded on the hologram. Therefore, in order to count accurately the number of droplets and determine their geometrical sizes, following the conditions that a given droplet can be analysed only once, some appropriate principles should be defined. If the droplet appears in the plane of image sharpness, its image on the TV screen is sharp and distinct and with the zero fringe in the centre of the droplet, which is narrower surrounded by a bright fringe. By combining the rule described and the one way tunneling recommended above the same droplet cannot be counted more than once. The droplets located in front of or behind the image plane, and appearing on the screen of the TV monitor are unsharp and diffused, being surrounded by a series of concentric diffraction fringes. The contours of such droplets are diffused, thus it is difficult to determine their sizes and real shape. Based on the examination carried out, it has been stated that the droplets of the diameter or order of 20  $\mu\text{m}$  are almost always spherical, whereas the droplets of diameter above 60  $\mu\text{m}$  take the following shapes: lens-like, elliptical, elongated rods. According to the author, this rule is valid for small pressures of atomizer feeding, whereas for higher outflow velocities from the atomizer the stream desintegrates into droplets more quickly, due to the dominant influence of the aerodynamic forces. It should be expected that in this case spherical shapes will be taken by droplets of diameter less than 20  $\mu\text{m}$ .

Till now, the reconstructed droplets have been recorded in the way given in [1, 4, 5]. The range of the droplet diameters was divided into intervals 20  $\mu\text{m}$  wide, and the droplet was recorded in such a way that its existence within



the given diameter interval was symbolized, its real diameter not being reported. According to the method of droplet recording elaborated by the author [3], for examinations of atomization in the internal combustion engine the spectrum of the droplet diameters is divided into intervals 10  $\mu\text{m}$  wide. Next, the droplet diameter is to be measured on the TV monitor and the measured value written in the given interval. The differences resulting from the comparison of the hologram analysis made according to the literature and the author's methods are significant, especially those for equivalent diameters (Fig. 5). This figure

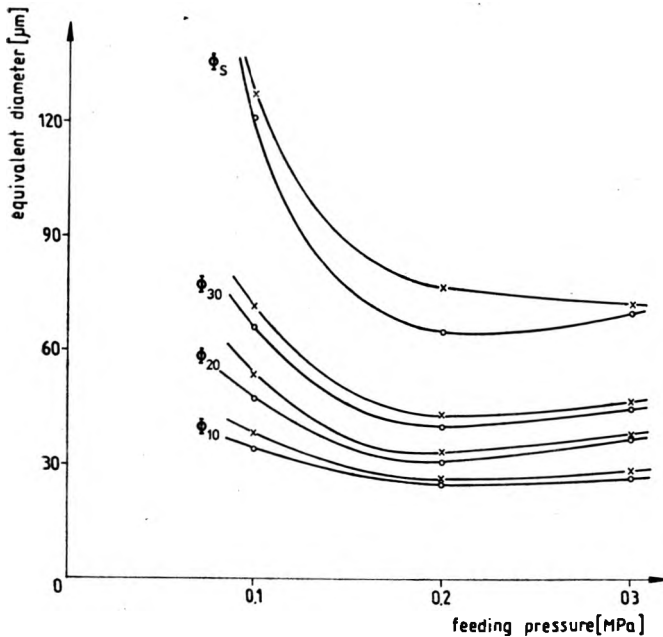


Fig. 5. Equivalent diameters of the droplets vs. the feeding pressure of the whirling atomizer ( $\times$  - acc. to the author,  $\circ$  - acc. to the literature)

shows the equivalent diameters, calculated according to both the literature method and that proposed by the author, vs the feeding pressure. The equivalent diameters evaluated according to the method suggested in this work are within the interval  $\Delta n_i$  greater by 2–10  $\mu\text{m}$  than those calculated by using the method of average diameter. Here 2–5  $\mu\text{m}$  refer to the arithmetical ( $\Phi_{10}$ ), surface ( $\Phi_{20}$ ), volume ( $\Phi_{30}$ ) diameters, while 10  $\mu\text{m}$  refers mainly to the Sauter diameter  $\Phi_S = \Phi_{32}$ . For the two kinds of atomizer sizes, the results of the equivalent diameters calculations and the standard deviations have been tabularized and will be presented in the next section of this paper.

As far as the quality of the atomization spectrum analysis is concerned, it is very essential to reduce the width of the interval  $\Delta n_i$  from 20  $\mu\text{m}$  to 10  $\mu\text{m}$ . Some examples of the atomization spectrum (the whirling atomizers examined by the author) plotted according to the literature method and to that proposed by the author are presented in Fig. 6. As is easily seen, the narrowing of the interval of droplet diameter to 10  $\mu\text{m}$  made it possible to find and emphasize the

real run of spectrum curve. The application of the proposed method enabled the author to observe very distinctly the local maxima of the distribution as well as a high deviation of the real spectrum run from the theoretical curve. The atomization spectrum according to [2] is presented in Fig. 7. These authors

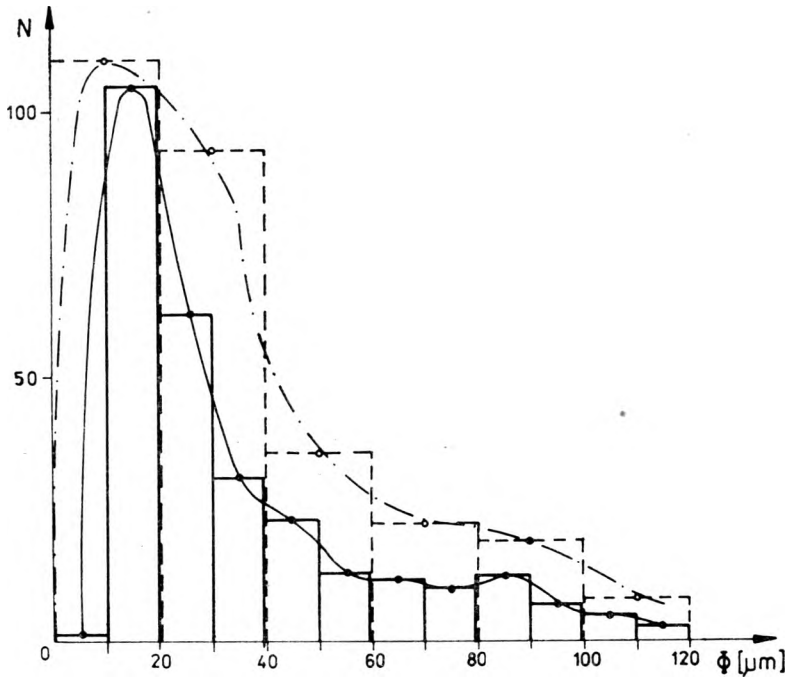


Fig. 6. Comparison of the water atomization spectra, plotted by the method given in the literature and that proposed by the author (— acc. to the author, - . - . - acc. to the literature).  $N$  — droplet number,  $\Phi$  — droplet diameter

divided the intervals of the droplet diameter irregularly so that the width of the interval  $\Delta n_i$  increased with the diameter of the measured droplets, while the number of droplets within this interval diminished. The droplet diameter on the TV monitor was not measured either. It is believed that the application of such great widths of the intervals  $\Delta n_i$  (up to 60  $\mu\text{m}$ ), each containing a small number of droplets, is too great a generalization and makes impossible the observation of the real run of the spectrum. As it may be seen from Fig. 7, the authors failed to obtain on the graph the local maxima of the distribution and the curve reported by them is close to the theoretical one.

## 5. Results of examinations of the water atomization spectrum from the whirling atomizers

Two types of whirling atomizers differing in sizes were examined. The water stream holograms were performed for each type and for different values of the feeding pressure. In this work, the holograms were analysed for feeding pressures

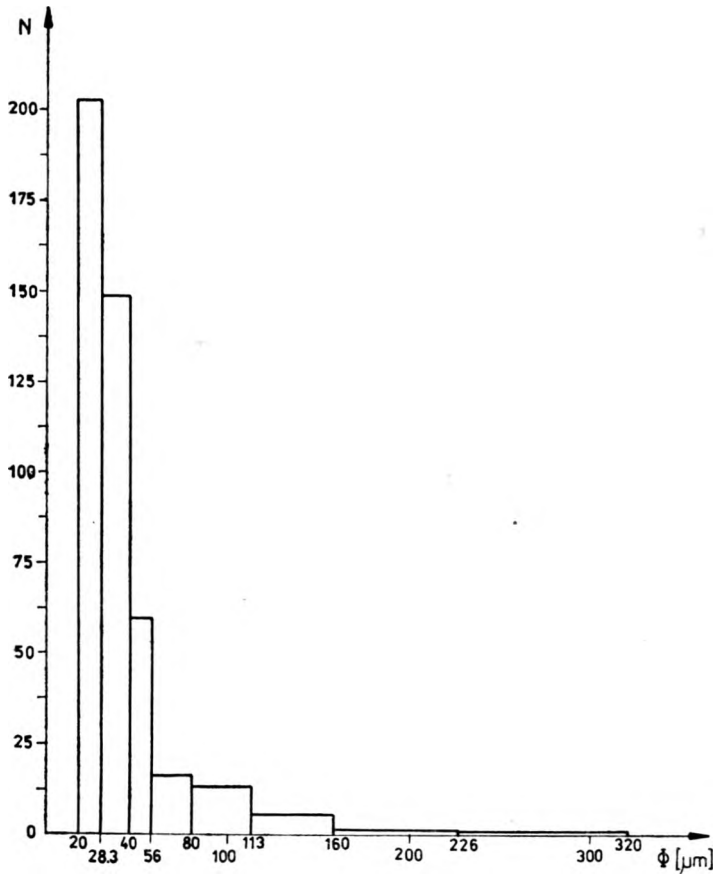


Fig. 7. Atomization spectrum according to [2],  $N$  - droplet number,  $\Phi$  - droplet diameter

Results of equivalent diameter and standard deviation calculations

Size	Large size atomizer		Small size atomizer		
	0.2 MPa	0.3 MPa	0.1 MPa	0.2 MPa	0.3 MPa
Feeding pressure	0.2 MPa	0.3 MPa	0.1 MPa	0.2 MPa	0.3 MPa
	0.2 MPa	0.3 MPa	0.1 MPa	0.2 MPa	0.3 MPa
$\Phi_{10}$	37.49	34.83	36.79	25.59	29.08
	37.46	34.09	33.49	25.06	28.77
$\Phi_{20}$	48.17	44.90	53.92	33.05	37.14
	47.59	45.02	48.71	31.74	37.02
$\Phi_{30}$	59.80	56.68	71.88	43.58	46.31
	58.87	56.82	66.29	40.46	46.19
$\Phi_S = \Phi_{32}$	92.13	90.33	127.77	75.77	72.01
	90.08	90.08	122.78	65.74	71.92
Standard deviation	30.28	28.37	39.53	20.94	23.13
	29.39	29.61	35.49	19.49	23.33

The upper values are calculated according to the method proposed by the author

of values: 0.1, 0.2 and 0.3 MPa. The results of equivalent diameter calculations are shown in the Table. The calculations of the upper values were based on the proposed method of hologram analysis, while the lower values were obtained by using the literature methods. In Figures 8–12 the atomization spectra are

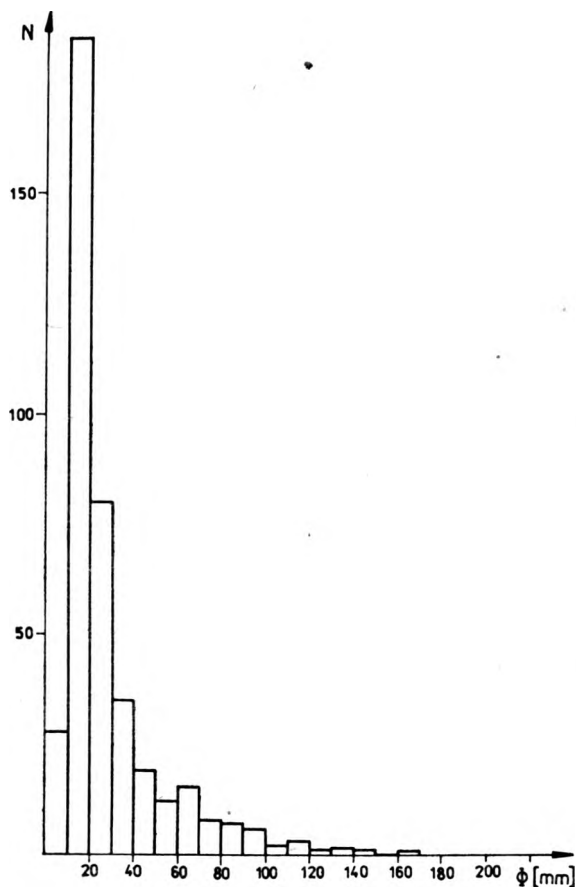


Fig. 8. Water atomization spectrum. Small size atomizer, feeding pressure 0.3 MPa.  $N$  – droplet number,  $\phi$  – droplet diameter measured with TV monitor

plotted, the analysis of the hologram being performed by using the author's method.

The dependence of the number of droplets upon the distance from the atomizer outlet is shown in Figs. 13 and 14. In each graph this dependence was compared for both the sizes of the atomizer and for a definite feeding pressure. The said dependence for the pressure 0.2 MPa is shown in Fig. 13. For the large atomizer the number of droplets decreases with the distance from the atomizer outlet, this decrease of the droplet number is, however, slight for the distance ranging between 15–22 mm. For the small atomizer the situation is quite opposite. The number of droplets rapidly drops for 15–20 mm distance from the atomizer outlet, and increases rapidly for the distances ranging from 22 to 29 mm. These observations may be explained by the fact that in the larger

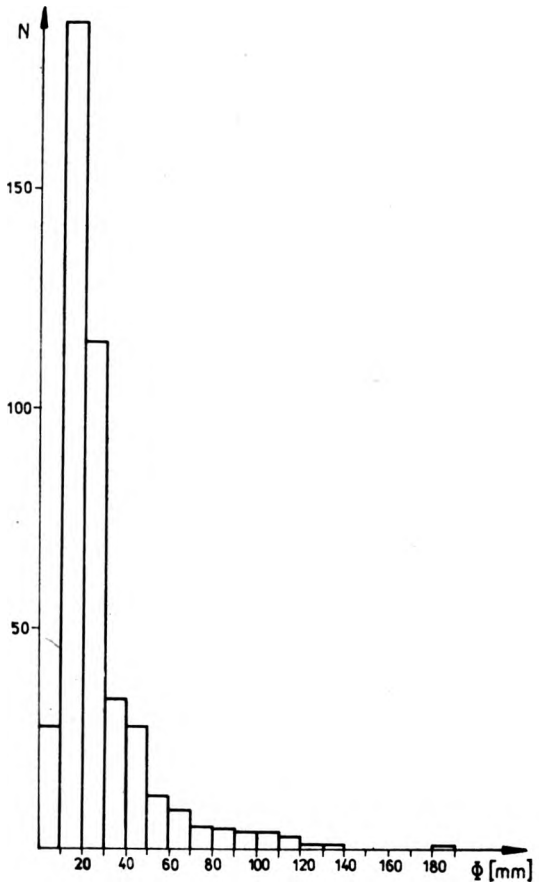


Fig. 9. Water atomization spectrum. Small size atomizer, feeding pressure 0.2 MPa.  $N$  - droplet number,  $\phi$  - droplet diameter measured with TV monitor

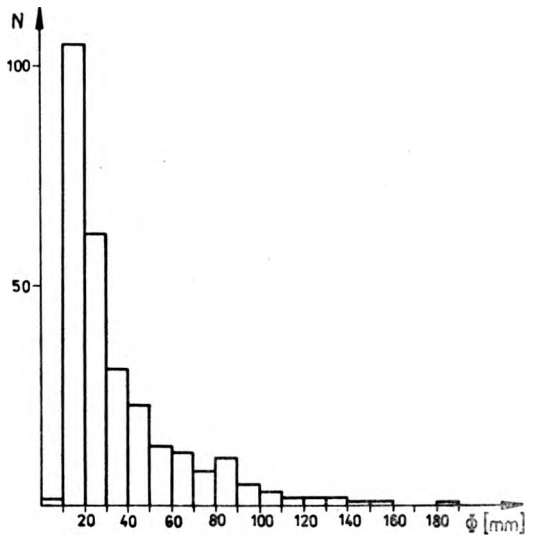


Fig. 10. Water atomization spectrum. Small sized atomizer, feeding pressure 0.3 MPa.  $N$  - droplet number,  $\phi$  - droplet diameter measured with TV monitor

atomizer the droplets are greater and they appear distinctly at the distance from the outlet ranging between 22 and 29 mm, while in the smaller atomizer small droplets are more characteristic at the distances between 22 and 29 mm. In Figure 14 the analysed dependence is shown for the pressure 0.3 MPa. For a large atomizer the number of droplets increases with the distance from the atomizer outlet, this increase being violent for the distances ranging from 15

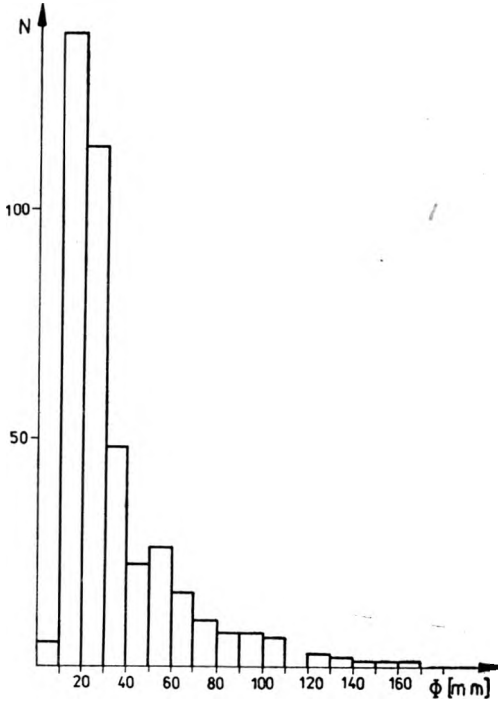


Fig. 11. Water atomization spectrum. Large size atomizer, feeding pressure 0.2 MPa.  $N$  – droplet number,  $\Phi$  – droplet diameter measured with TV monitor

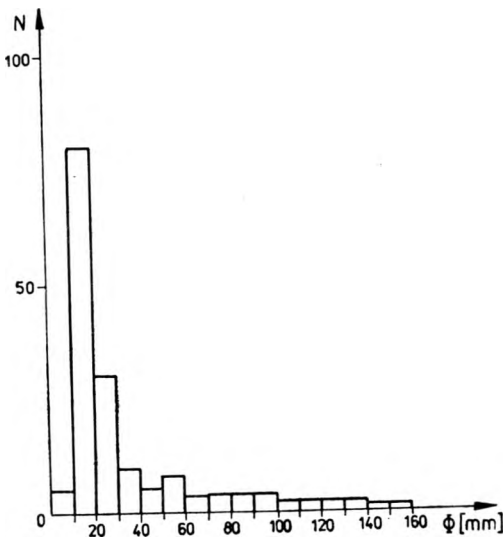


Fig. 12. Water atomization spectrum. Small size atomizer, feeding pressure 0.1 MPa.  $N$  – droplet number,  $\Phi$  – droplet diameter measured with TV monitor

to 22 mm, and a very slight one within the distance interval of 22–29 mm. A continuous increase of the droplet number with the increasing distance from the atomizer was also observed for the small atomizer. Within the 15–22 mm interval this dependence is almost a linear one and in this case small droplets dominate within the whole range of analysed distances. For the large atomizer –

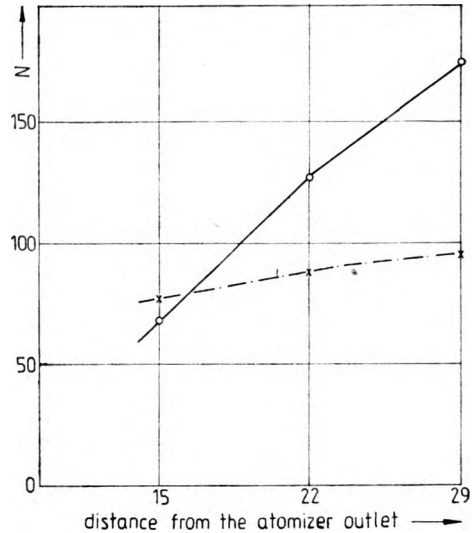
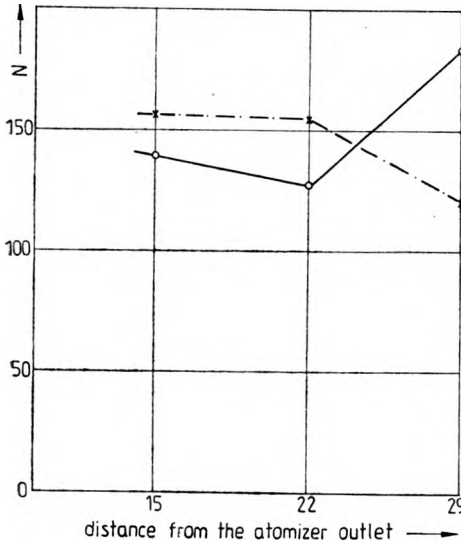


Fig. 13. Quantity of the droplets vs. their distance from the stream atomizer outlet, for the pressure 0.2 MPa (x – large size atomizer, o – small size atomizer)

Fig. 14. Quantity of the droplets vs. their distance from the stream atomizer outlet, for the pressure 0.3 MPa (x – large size atomizer, o – small size atomizer)

– the droplets are large, no especially numerous population of great droplets being observed for the distances of 20–29 mm. In the plotted atomization spectra (Figs. 8–12) the existence of a distinct additional local maximum draws attention.

## 6. Suggested application of laser holography to examination of the atomization spectrum in an operating engine

The considerations presented in this part of the paper are essentially a proposition of applying the holographic method to examinations of atomization spectra in the working engine, to which a testing engine SB 3.1 is intended to be adjusted. The main problems connected with the application of a holographic system to a working engine are:

i) Vibrations of the setup which influence disadvantageously the formation of the interference pattern, since they may cause the shift of the fringes and even make impossible the formation of the holographic image. In order to eliminate the influence of engine vibrations on the image formation, a pulse ruby laser

of pulse duration of orders of  $10^{-9}$  s is supposed to be applied in these examinations.

ii) Long way of the travelling laser beam requires a high spatial coherence, which is very difficult to assure when such short pulses are applied. Therefore, the optical paths of the object and reference beam should be equal (Fig. 15).

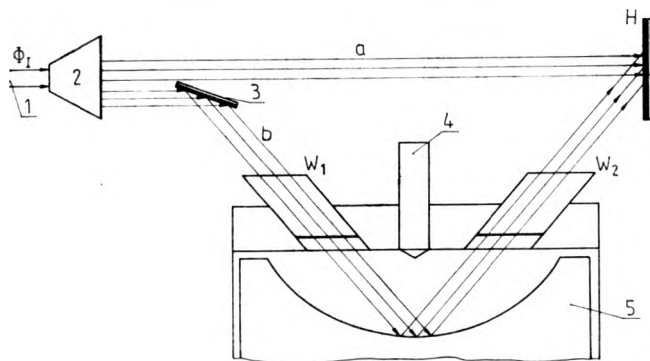


Fig. 15. Suggested application of the holographic system in examinations of fuel on a working engine (1 – laser beam, 2 – laser beam expander, 3 – mirror, 4 – atomizer, 5 – piston). For the others notations, see the text

iii) A closed and nontransparent system including the combustion chamber which necessitates viewing of this system. This means that two viewers of diameter of about 20 mm, equipped with quartz window in the head of the engine are required.

iv) Quartz windows mounted in the viewers  $W_1$  and  $W_2$  (Fig. 15) which are exposed to the operation of high pressures and temperatures. These phenomena may cause the cracking of the quartz cylinders and thus the pollution of the droplet image, due to the surface and internal stresses in the quartz.

Keeping in mind the above remarks a scheme of the examination setup of two-beam type has been presented in Fig. 15. A beam  $\Phi_I$  emerges from the pulse ruby laser. In the optical system 2, it is split into reference and object beams. Each of them is widened to the requested diameter. The reference beam **a** falls immediately on the holographic plate **H**, while the object beam **b** is directed through an optical system to the combustion chamber via a viewer. The light beam, after having been reflected from the piston bottom, falls also onto the holographic plate where it interferes with the reference beam. The beam **b** during its run through the combustion chamber passes through the injected stream of fuel.

The SB 3.1 engine proposed for examinations has a toroidal combustion chamber, a partial cut out of the toroid ascent is foreseen in order to facilitate the light reflectance from its bottom. It is believed that such examinations will allow us to recognize the real run of the stream desintegration and enable the recognition of the distribution of both the quantity and the sizes of droplets, within the volume of the combustion chamber.



## 7. Concluding remarks

Summing up the considerations presented in this work, it may be stated that the selection of the suitable method for the analysis of droplet hologram has an essential influence on the quality of the obtained results. The analysis of droplet was performed having in mind the atomization spectrum, which has been accepted as a characteristic quality feature of the fluid atomization from the atomizers of various types. The second part of the paper deals with a practical role of the atomization spectrum for the fuel-air mixture, formed in the ZS engine of direct injection.

A particular attention is payed to the influence of the method of hologram analysis on the calculation accuracy of the equivalent diameters of the droplets, especially of the Sauter diameters, as it is very essential in calculations concerning the physico-chemical and heat processes. The method of holograms analysis, proposed by the author, gives more accurate results than the other methods described in the literature. It makes it possible, moreover, to observe the run of the local maxima of the spectrum, illustrated distinctly in the section presenting the result of examinations concerning the water whirling atomizers. The analysis of the Figs. 8-12 makes it possible to observe that for different pressures and for two sizes of atomizers the maximum of the distribution occurs for the same diameter of the droplets. This conclusion is not fully confirmed by statistical analysis, since only several dozen measurements of the parameter pairs (atomizer-size-feeding pressure) were performed. Nevertheless, the conclusion formulated in this work signals the probability of the existence of such a relation. Based on the analysis of the presented results it has been stated that under the same pressure conditions an increase in the atomizer size (of the same type) results in a higher percentage of large droplets. In the last section, an application of the holographic method to examination of fuel atomization spectrum on a working SB 3.1 engine is suggested.

*Acknowledgements* - The author is indebted to Prof. Z. Orzechowski and Eng. G. Kowalewski from the Institute of Flow Machines, Technical University of Łódź, for rendering accessible their lab and the aid in performing the examinations.

## References

- [1] KOZIKOWSKA A., *Acta Geophys.*, **26** (1978), 3.
- [2] POLYMEROPOULOS C. E., SERNAS V., *Comb. a. Flame* **29** (1977), 123.
- [3] WĘCLAŚ M., *Proc. Conf. Autoprogress 83/84*, Jadwisin 1984, Vol. 3.
- [4] RIECK H., *Proc. Symp. Eng. Uses of Holography*, Cambridge University Press 1970.
- [5] BRIONES R. A., HEFLINGER L. O., WUERKER R. F., *Appl. Opt.* **17** (1978).
- [6] DE VELLIS J. B., REYNOLDS G. O., *Theory of Application of Holography*, Addison Wesley, Massachusetts 1967.
- [7] PAVITT K. W., JACKSON M. C., ADAMS R. J., BARTLETT J. G., *J. Phys. E: Sci. Instr.* **3** (1970), 971.

[8] THOMPSON B. J., J. Phys. E: Sci. Instr. 7 (1974), 781.

[9] ВЕХОН R., J. Phys. E: Sci. Instr. 6 (1973), 245.

*Received September 6, 1984,  
in revised form March 1, 1985*

### **Метод анализа голограмм распыливаемой жидкости для определения спектра распыления**

Приведены методы регистрации и анализа голограмм распыливаемой жидкости. Представлен новый метод анализа голограмм и сравнен с другими методами. Дан анализ спектра распыления для водяных распылителей. Определены диаметры капель и их множество.